The rate of heat transfer to the coolant surface was approximated by

$$\dot{Q} = U_H A\left[\frac{(T_I+T_o)}{2} - T_s\right]$$

where: $\dot{Q}$ = heat flow rate, Btu/sec, U_H = heat transfer coefficient, Btu/in.^{2}-sec-°F, A = exposed coolant surface (in.^{2}), and $(T_I+T_o)/2$ = average gas temperature in coolant bed, °R. The combination of gases exiting through a nozzle (or into a turbine) is given by

$$\dot{m}_g+\dot{m}_c = C_{D_m} A_t P_o$$

where: C_{D_m} = discharge coefficient of gas mixture, sec^{-1}, A_t = nozzle area, in.^{2}, and P_o = filter/cooler outlet pressure, psi.

To compare various candidate coolant materials analytically, a rating parameter was generated. This parameter, designated specific energy, is given by

$$\text{specific energy} = \frac{KT_m}{MW_m}\left(\frac{\gamma_m}{\gamma_m-1}\right)\left[1-\left(\frac{P_a}{P_o}\right)^{(\gamma_m-1)/\gamma_m}\right]$$

where: K = dimensionless constant, T_m = mixture gas outlet temperature, °R, MW_m = molecular weight of gas mixture, lb-mole/lbm, γ_m = specific heat ratio of mixture, P_a = ambient pressure, psi, and P_o = filter/cooler outlet pressure, psi.

DECEMBER 1974 J. SPACECRAFT VOL. 11, NO. 12

Damping of Axial Instabilities by Small-Scale Nozzles Under Cold-Flow Conditions

B. A. JANARDAN,* B. R. DANIEL,* AND B. T. ZINN†
Georgia Institute of Technology, Atlanta, Ga.

The damping of axial instabilities by a variety of small-scale solid rocket nozzles has been determined experimentally under cold-flow conditions using the modified impedance tube technique. The dependence of the damping upon the cavity depth and the secondary flow rate issuing from the cavity of a submerged nozzle, the geometry of the convergent section of a single-ported nozzle, and the number of nozzles present in a multiple-ported nozzle cluster has been determined. Measured data indicate that in the case of the submerged nozzle the cavity depth surrounding the nozzle has a significant effect upon the nozzle admittance while the secondary flow rate issuing from the cavity has negligible effect on the admittance. Tests conducted with conical, equal-radii-of-curvature and linear-velocity-profile nozzles showed that conical nozzles provide the most damping. Tests with multiple-ported nozzles indicated that quadruple-ported nozzles provide less damping for axial instabilities than single and dual-ported nozzles whose damping capabilities are approximately the same.

Nomenclature

A = amplitude of pressure oscillation, psfa (rms)
$\hat{A}$ = constant
c = velocity of sound, fps
f = frequency, Hz
F = nondimensional frequency defined as equal to $\omega r_c/\bar{c}$
i = imaginary unit, $(-1)^{1/2}$
L = length, ft
M = Mach number
p = pressure, psfa
P = pressure amplitude, psfa (rms)
q = secondary to primary flow rate ratio
r = radius, ft
S = cross-sectional area, ft^2
T = period of oscillation, sec
u = axial velocity, fps
V = volume, ft^3
y = nondimensional admittance, defined by Eq. (8)
Y = admittance, defined by Eq. (7), ft^3/lbf-sec
z = axial coordinate
α = nozzle admittance parameter, defined by Eq. (5)
α_N = nozzle decay coefficient, defined by Eq. (15), sec^{-1}
β = nozzle admittance parameter, defined by Eq. (6)
γ = specific heat ratio
Γ = real part of nondimensional admittance
δ = pressure phase, defined by Eq. (14), rad
η = imaginary part of nondimensional admittance
λ = wavelength, ft
Λ = nondimensional decay coefficient
ρ = density of gas in the chamber, lbf-sec^2/ft^4
ω = angular frequency, rad/sec

Superscript
$\bar{(\ )}$ = steady-state quantity

Subscripts
c = denotes a chamber property
N = quantity related to nozzle behavior
1 = perturbed quantity

Presented as Paper 73-1223 at the AIAA/SAE 9th Propulsion Conference, Las Vegas, Nev., November 5–7, 1973; submitted November 28, 1974; revised June 10, 1974. This research was supported by Air Force Rocket Propulsion Laboratory, Edwards Air Force Base, Calif., under Contract F04611-71-C-0054. The authors acknowledge the assistance given by W. A. Bell and A. J. Smith Jr. during the course of this research.

Index categories: Combustion Stability, Ignition, and Detonation; Solid and Hybrid Rocket Engines.

* Research Engineer.

† Regents' Professor of Aerospace Engineering. Associate Fellow AIAA.

Introduction

SOLID propellant rocket motors are often subject to combustion instabilities involving oscillations of the gases within the combustion chamber. Such instabilities can result in failure of

the rocket motor and the mission due to large-amplitude pressure oscillations, increased heat transfer rates and severe vibrations of the engine structure. Several techniques have been used to suppress the instabilities. Among these, the employment of powdered metals or metallic oxides in the solid propellant[1] has proven effective in the suppression of high-frequency combustion instability. However, experience with large size rocket motors (e.g., see Refs. 2 and 3) has indicated that such additives do not necessarily suppress the intermediate-frequency axial combustion instability. Currently, no reliable technique exists for suppressing this type of instability. Hence suppressing intermediate-frequency axial combustion instability is currently a major consideration in the design and development of large solid rocket motors.[3]

This paper is concerned with the quantitative evaluation of the capabilities of various solid rocket nozzle designs to attenuate axial instabilities in the intermediate-frequency range. To evaluate nozzle damping, the admittance at the nozzle entrance plane must be determined. The admittance is also needed in linear stability analyses where it is used as the boundary condition that must be satisfied at the nozzle end of the combustion chamber.

The theoretical determination of the nozzle admittance is a difficult gas dynamical problem which requires the solution of a mathematically complex system of conservation equations which describe the behavior of the flow oscillations in the convergent section of a choked nozzle. Available theoretical treatments for computing the nozzle admittance are complex in nature, and, to date, solutions have been obtained only for a limited number of cases. The most sophisticated treatment of the nozzle admittance problem was developed by Crocco and Sirignano[4] who considered the case where the wave motion in the nozzle is three-dimensional and the mean flow is one-dimensional. The latter assumption implies a slowly converging nozzle. This theoretical treatment is also applicable to cases where both the wave motion and the steady-state flow are one-dimensional and it can be used to predict the behavior of short nozzles; the latter case is covered in more detail in Refs. 5 and 6. These theoretical treatments are, however, applicable to nozzles having simple geometrical configurations and one must resort to experimental studies whenever the admittances of complex nozzle designs are needed.

There are several experimental techniques that could be used to determine the damping capabilities of a nozzle. They are referred to as the direct, wave-attenuation, frequency-response, and the modified impedance-tube technique. In the direct technique[7] a hot-wire anemometer probe and a pressure transducer are installed in the entrance plane of the nozzle. The nozzle admittance is determined from direct measurements of the amplitudes and phases of the axial flow velocity and pressure oscillations at the nozzle entrance plane. In the wave-attenuation technique[8] a pressure pulse is superimposed on a steady flow in a simulated rocket combustion chamber by bursting a diaphragm at the upstream end of the chamber. The decay rate of the resulting pressure pulse is measured and this data is used to determine the nozzle admittance. In the frequency-response technique[8] an acoustic wave of a known frequency is excited in a simulated rocket combustion chamber. The frequency of the oscillations is slowly varied over a range of frequencies starting with a frequency below one of the resonant frequencies of the chamber and ending at a frequency above the chosen resonant frequency. The amplitudes of the resulting pressure oscillations are measured and plotted as a function of the driving frequency. From the shape of the resulting acoustic response curve, the nozzle admittance at the chosen resonant frequency can be determined. The modified impedance-tube technique is an extension of the classical no-flow impedance-tube method[9] employed to measure the acoustical damping capabilities of various materials. In the modified impedance-tube technique, a sound source capable of generating simple harmonic waves of desired frequencies is placed at one end of a simulated rocked chamber. The other end of the chamber is attached to the nozzle whose admittance is to be determined. With the aid of the acoustic driver, a standing-wave pattern of a known frequency is superimposed upon the one-dimensional mean flow present in the chamber. The admittance of the nozzle is determined by measuring the amplitudes and phases of the resulting standing waves by means of a set of microphones located along the chamber walls.

The applicability of the various techniques for measuring nozzle admittances has been investigated by Culick and Dehority.[10] One of the important results of this study has been the conclusion that the impedance-tube method appears to be the most suitable for the measurement of nozzle admittances. A similar conclusion has also been reached independently by Bell.[11] References 10 and 11 derive the equations and discuss the experimental setup required to measure nozzle admittances in an impedance tube containing a steady one-dimensional flow. The applicability of this technique has been established by Zinn et al.[12] who used it to experimentally determine the admittances of liquid propellant rocket nozzles subjected to three-dimensional pressure oscillations. Based on the preceding results and recommendations, it had been decided to use the modified impedance tube technique in this study to determine the damping provided by various solid rocket nozzle designs.

Analytical Considerations

Nozzle Admittance

A qualitative description of the theory and a summary of the relevant expressions required for the nozzle admittance measurements, using the modified impedance-tube technique, are presented here (see Ref. 11 for details). The required expressions are obtained by solving the system of conservation equations that describe the behavior of small amplitude, one-dimensional disturbances which are superimposed upon a steady one-dimensional flow inside a simulated cold-flow rocket combustor having an acoustic driver at one end and a choked nozzle at the other. The previously mentioned solutions are then required to satisfy the admittance boundary condition at the nozzle entrance. The resulting expressions describing the time and space dependence of the pressure and velocity perturbations inside the simulated combustor are given below:[11]

$$p_1(z,t) = \gamma \bar{p} \hat{A}\, e^{i(\omega t + az)} \cosh(\phi - iRz) \tag{1}$$

$$u_1(z,t) = \bar{c} \hat{A}\, e^{i(\omega t + az)} \sinh(\phi - iRz) \tag{2}$$

where

$$R = \frac{(\omega/\bar{c})}{(1-\bar{M}^2)}; \qquad a = R\bar{M}$$

$$\phi = \pi\alpha - i\pi\left[\beta + \frac{2(L_c - z)}{\lambda} + \tfrac{1}{2}\right] \tag{3}$$

and

$$\lambda = 2\pi(1-\bar{M}^2)/(\omega/\bar{c}) \tag{4}$$

The two parameters α and β, respectively, describe[13] the changes in amplitude and phase between the incident and reflected pressure waves at the nozzle entrance; that is,

$$\left(\frac{\text{Amplitude of reflected pressure wave}}{\text{Amplitude of incident pressure wave}}\right)_{\substack{\text{nozzle}\\ \text{entrance}}} = e^{-2\pi\alpha} \tag{5}$$

$$\left(\text{Phase change between incident and reflected pressure waves}\right)_{\substack{\text{nozzle}\\ \text{entrance}}} = \pi(1+2\beta) \tag{6}$$

where parameter β must satisfy $|\beta| \leqq 0.5$.

The specific nozzle admittance, Y_N, is defined as

$$Y_N = u_1/p_1 \tag{7}$$

In general, the nozzle admittance is a complex number whose real and imaginary parts describe the relationships that exist at the nozzle entrance between the amplitudes and phases of the

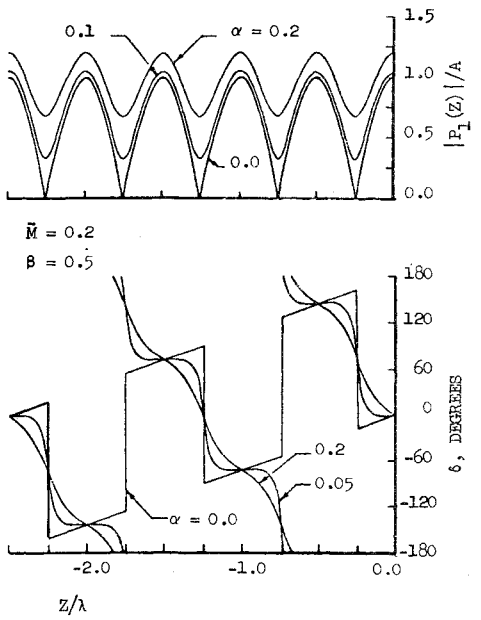

Fig. 1 Pressure amplitude and phase distribution along a modified impedance tube.

velocity and pressure perturbations. These relationships depend upon the wave motion inside the convergent section of the nozzle. The nondimensional form of the specific nozzle admittance is written in the following form:

$$y_N = \frac{Y_N}{Y_g} = \bar{\rho}\bar{c}\left(\frac{u_1}{p_1}\right)_{z=0} = \Gamma + i\eta \tag{8}$$

where the reference admittance $Y_g = (1/\bar{\rho}\bar{c})$ is the characteristic admittance of the gas medium in the chamber. Substituting the solutions obtained for the pressure and velocity perturbations [i.e., Eqs. (1) and (2)] into the above definition yields the following expression for the nondimensional nozzle admittance y_N:

$$y_N = \coth \pi(\alpha - i\beta) \tag{9}$$

Separating the nondimensional nozzle admittance into its real and imaginary parts, the following relations are obtained:[11]

$$\Gamma = \frac{\tanh(\pi\alpha)\sec^2(\pi\beta)}{\tanh^2(\pi\alpha)+\tan^2(\pi\beta)} \tag{10}$$

$$\eta = \frac{\operatorname{sech}^2(\pi\alpha)\tan(\pi\beta)}{\tanh^2(\pi\alpha)+\tan^2(\pi\beta)} \tag{11}$$

Examination of Eqs. (8) through (11) shows that the nondimensional nozzle admittance depends upon the steady-state properties of the flow and the parameters α and β.

The parameters α and β can be evaluated from pressure amplitude or phase measurements inside a simulated, cold-flow rocket combustor. To accomplish this, Eq. (1) is rewritten in the following form:

$$p_1(z,t) = |P_1(z)|\, e^{i(\delta+\omega t)} \tag{12}$$

where the pressure amplitude $|P_1(z)|$ and pressure phase δ are given by

$$|P_1(z)| = A\left[\cosh^2(\pi\alpha) - \cos^2\pi\left\{\beta + \frac{2z}{\lambda}\right\}\right]^{1/2} \tag{13}$$

$$\delta(z) = az + \arctan\left[\tanh(\pi\alpha)\cot\pi(\beta + 2z/\lambda)\right] \tag{14}$$

Equations (13) and (14) show that the pressure amplitude and phase are functions of the axial coordinate, the steady-state properties of the medium, the known frequency and the unknowns α, β, and A. The availability of such expressions for the pressure amplitude and phase suggest that if one can measure the pressure amplitude and/or pressure phase at three different locations along the chamber, then the experimental data could be substituted into Eq. (13) and/or Eq. (14) and the resulting algebraic equations could then be solved to determine the parameters α and β. In this investigation the admittance parameters α and β were determined by measuring *both* the pressure amplitudes and phases. The resulting values of α and β were then substituted into Eqs. (9–11) to determine the nozzle admittance.

Since the expressions relating $|P_1|$ and δ to the admittance parameters α and β are nonlinear, pressure amplitude or phase measurements taken at only three discrete axial locations may not guarantee the uniqueness and accuracy of the calculated values of α and β. Stated differently, pressure amplitude or phase measurements taken at three locations will not yield enough information about the shape of the standing wave pattern inside the simulated combustor. This point is made clearer by studying the plots (e.g., see Ref. 14) describing the axial distributions of the pressure amplitudes and phases for various values of $\bar{M}$, α, β, and the wavelength λ. A typical plot is shown in Fig. 1.

To improve the accuracy of the measured admittances, 10 transducers placed at different locations along the modified impedance tube were used during this investigation. The unknown admittance parameters were then obtained by using the nonlinear regression technique[11] which determines the set of values of α and β that minimizes the rms deviation between the measured pressure amplitudes and/or phases and the corresponding expressions as given by Eqs. (13) and (14). Additional details on the use of this technique are given in Ref. 11.

Nozzle Decay Coefficient

In practice,[15] the over-all stability of solid propellant rocket motors is often determined by evaluating a coefficient α_{gd} that describes the rate of growth or decay of a small-amplitude oscillation inside the combustor. The sign of α_{gd} determines whether the oscillation will grow or decay with time. The coefficient α_{gd} can be expressed as a summation, $\sum_i \alpha_i$, where the components α_i represent the contributions of the various relevant processes (e.g., combustion, the nozzle) to the stability of the rocket combustor. This section is concerned with the evaluation of the quantity α_N that may be regarded as a measure of the damping provided by the nozzle. When the nozzle is the only factor that can affect the growth or decay of an oscillation inside the combustor, the temporal behavior of the combustor oscillation may by expressed in the following form:

$$p_1(z,t) = P(z)\, e^{\alpha_N t}\, e^{i\omega t} \tag{15}$$

The following discussion will outline how the measured nozzle admittance data can be used to measure the nozzle decay coefficient.

According to Ref. 16, the nozzle decay coefficient may be determined from the following relationship:

$$2\alpha_N \hat{V} = -\int_{\substack{\text{nozzle}\\ \text{entrance}}} dS\mathbf{n}\cdot\left\{p_1\mathbf{u}_1 + \frac{\bar{\mathbf{M}}}{\bar{\rho}\bar{c}}p_1^2 + \bar{\rho}\bar{c}(\bar{\mathbf{M}}\cdot\mathbf{u}_1)\mathbf{u}_1 + (\bar{\mathbf{M}}\cdot\mathbf{u}_1)p_1\bar{\mathbf{M}}\right\} \tag{16}$$

where

$$\hat{V} = \int_{\substack{\text{combustor}\\ \text{volume}}} dV\left\{\tfrac{1}{2}\bar{\rho}\mathbf{u}_1\cdot\mathbf{u}_1 + \tfrac{1}{2}\frac{p_1^2}{\bar{\rho}\bar{c}^2} + \frac{\bar{\mathbf{u}}\cdot\mathbf{u}_1}{\bar{c}^2}p_1\right\} \tag{17}$$

and the time average $\langle\ \rangle$ is defined as follows:

$$\langle\ \rangle = \lim_{T\to\infty}\frac{1}{T}\int_0^T (\ )\,dt$$

Implied in Eqs. (16) and (17) is the assumption that the growth or decay rate of the oscillations is small. It should also be pointed out that in order to evaluate the nozzle decay coefficient using Eqs. (16) and (17), the acoustic mode structure [i.e., $p_1(z,t)$ and $\mathbf{u}_1(z,t)$] and the steady-state flow conditions throughout the chamber must be known. Substituting the expression

for the nozzle admittance Y_N into Eq. (16) and rearranging yield the following expression:

$$2\alpha_N \hat{V} = -\int_{\substack{\text{nozzle}\\ \text{entrance}}} dS|P_N|^2[(1+\bar{M}^2)\,Re\{Y_N\}+ \frac{\bar{M}}{\bar{\rho}\bar{c}}+\bar{\rho}\bar{c}\bar{M}\,|Y_N|^2] \quad (18)$$

where $|P_N|$ is the amplitude of the pressure oscillation at the nozzle entrance. The relationships $\bar{\mathbf{M}}\cdot\mathbf{n}=\bar{M}$ and $\mathbf{u}_1\cdot\mathbf{n}=u_1$, where now $\bar{M}$ and u_1 should be interpreted as the components of the steady-state Mach number and velocity perturbation in the direction of the normal $\mathbf{n}$, were used in the derivation of Eq. (18). Assuming uniform flow conditions at the nozzle entrance plane, Eq. (18) can be rewritten as follows:

$$\left(\frac{2\bar{\rho}\bar{c}\hat{V}}{S_N|P_N|^2}\right)\alpha_N = -[(1+\bar{M}^2)\,Re\{y_N\}+\bar{M}+\bar{M}\,|y_N|^2] \quad (19)$$

The right-hand side of Eq. (19) consists of 4 terms, 3 of which depend upon the steady-flow Mach number at the nozzle entrance. These 3 terms may be considered as representing wave energy losses resulting from the presence of a mean flow and the remaining term is the radiative wave energy loss. Examination of Eq. (19) indicates that the decay coefficient can be determined from the knowledge of a) the specific acoustic impedance $\bar{\rho}\bar{c}$ of the medium, b) the nozzle entrance area S_N, c) the structure of the acoustic wave inside the combustor as represented by the parameter $\hat{V}/|P_N|^2$ and d) the values of $\bar{M}$ and y_N.

The scaling criteria that should be employed to obtain the admittance data of full-scale nozzles under "hot" conditions from the measured cold-flow, small-scale data has been investigated as a part of this study. The results of this scaling investigation will be reported in a separate publication.

Experimental Setup

The test apparatus includes a cold-flow acoustic test facility capable of simulating rocket engine combustion instabilities in a laboratory setup in which a wide range of test variables may be investigated. In the experimental setup, the rocket engine combustor is replaced by the modified impedance tube and the gas flow generated by the combustion process is simulated by a steady one-dimensional mean flow. The periodic oscillations in the unsteady combustor are reproduced by means of two electropneumatic acoustic drivers which generate discrete frequency pressure oscillation inside the modified impedance tube. A schematic diagram of the test facility is presented in Fig. 2.

Impedance Tube

The modified impedance tube used in this investigation has been specifically designed to investigate the acoustical damping capabilities of rocket engine exhaust nozzles. The impedance tube is $11\frac{3}{8}$ in. in diameter and 120 in. in length. The upstream end of the impedance tube is attached to an ejector plate and the test nozzle is coupled directly to the flange at the downstream end of the impedance tube. Provision has been made along the length of the impedance tube for the installation of acoustic drivers, dynamic pressure transducers, thermocouples, and static pressure orifices.

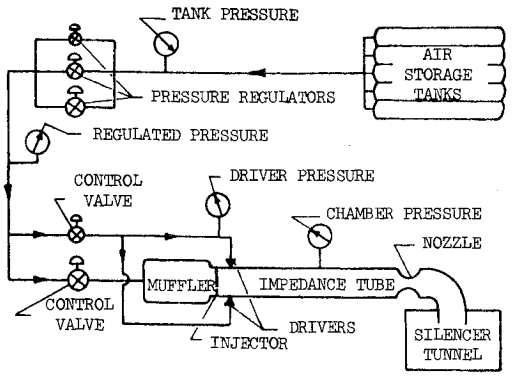

Fig. 2 Schematic diagram of the acoustic test facility.

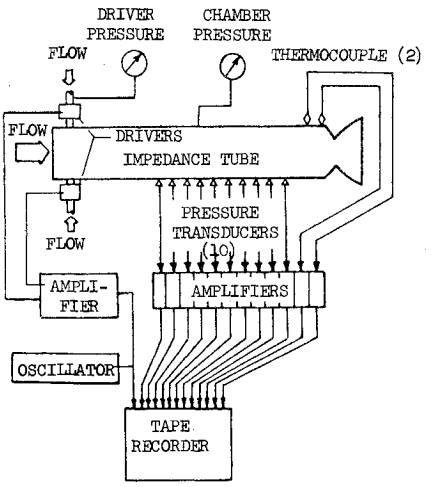

Fig. 3 Instrumentation diagram.

Instrumentation and Data Processing

A diagram of the instrumentation system used to monitor, regulate, measure, and record the conditions inside the modified impedance tube is shown in Fig. 3. During a test the frequencies of the driven waves were varied over the range of 40 Hz to 600 Hz at a rate of 8 Hz/sec. The analog data recorded on the tape recorder during each test were digitized by a 14 channel analog-to-digital conversion system. The digitized data were then numerically analyzed by means of a Fourier analysis to determine the amplitudes and phases of the chamber pressure oscillations as a function of the driver input frequency. The resulting pressure amplitudes and phases along with the measured temperature data were then used to determine the admittance parameters α and β and the real and imaginary parts of the nondimensional admittance of the tested nozzles.

Test Nozzles

The facility is restricted to testing nozzles and combustion chambers with cross section diameter no greater than $11\frac{3}{8}$ in., which is the inside diameter of the impedance tube. Hence, the damping provided by full-scale rocket nozzles has been determined by investigating the damping capabilities of geometrically similar small-scale nozzles.

In a typical application, a submerged nozzle is recessed into the combustion chamber where it is surrounded by the solid propellant grain, as shown in Fig. 4. After ignition, the recession of the burning propellant surface results in an increase with

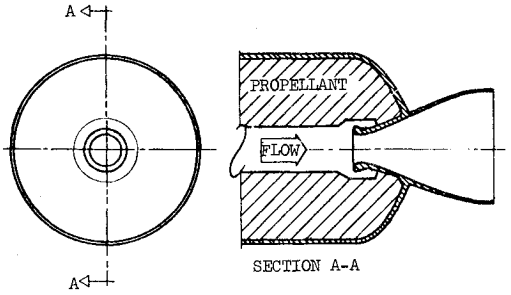

Fig. 4 Typical submerged rocket nozzle configuration.

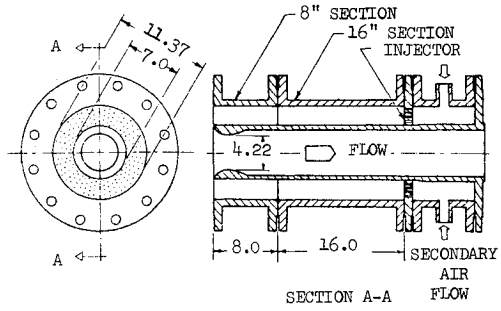

Fig. 5 Submerged nozzle test configuration.

time of the depth of the cavity surrounding the nozzle, and the flow rate of the combustion products flowing from the cavity into the chamber. In the present study the influence of the cavity depth and the cavity flow rate upon nozzle admittance has been investigated by using the test configuration shown in Fig. 5. The location of the secondary injector, which determines the cavity depth, can be varied in 8 in. increments from a position flush with the nozzle entrance plane to a position 24 in. aft of the nozzle entrance plane. This can be done by rearranging the location of the secondary injector with respect to the 8 in. and 16 in. interchangeable nozzle sections. The secondary injector is a porous plate designed to provide a uniform secondary airflow into the nozzle cavity. This injector has a high acoustic impedance which isolates the secondary airflow plenum chamber from the pressure oscillations in the nozzle cavity. In this study, the ratio of the secondary cavity

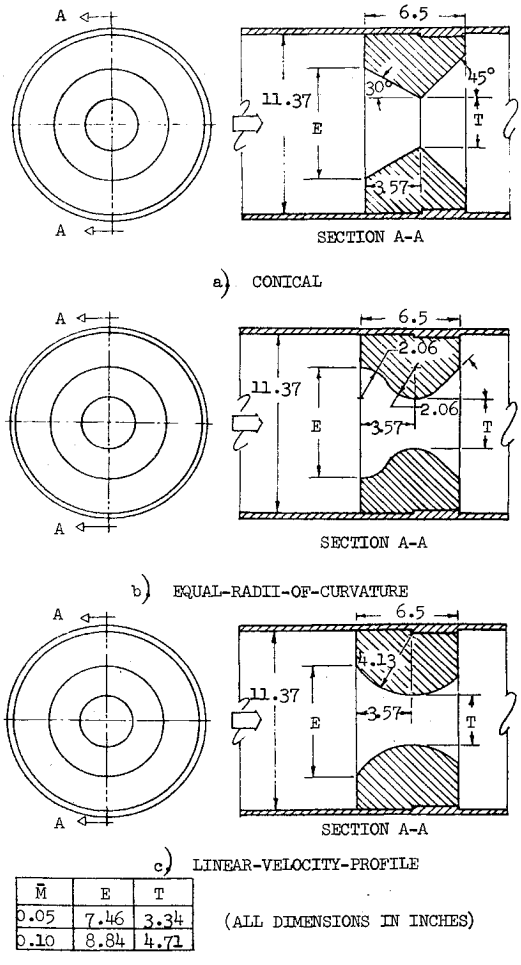

M	E	T
0.05	7.46	3.34
0.10	8.84	4.71

Fig. 6 Convergent section geometry of test nozzles.

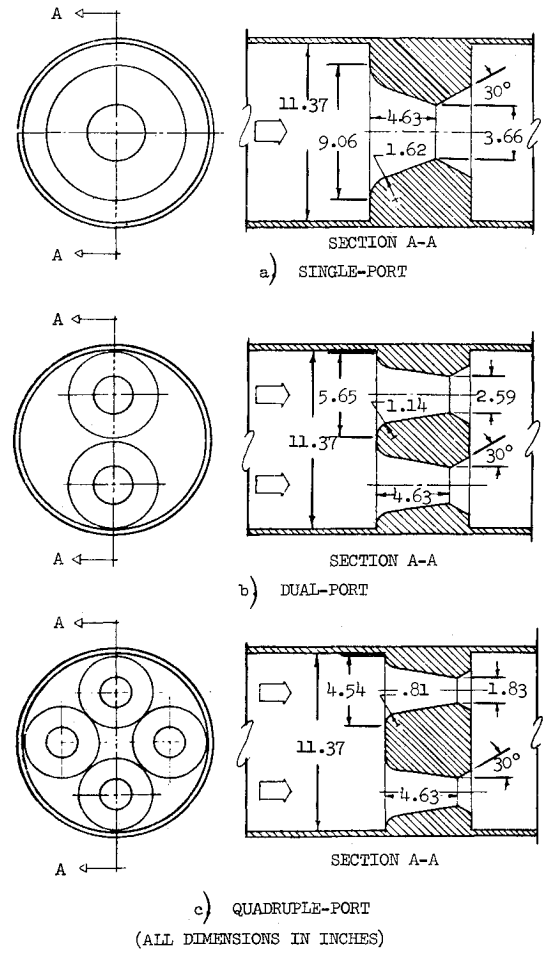

Fig. 7 Single- and multiple-ported test nozzles.

flow rate to primary chamber flow rate was changed between 0% and 25% in steps of 5%.

To investigate the dependence of nozzle damping upon the geometry of its convergent section, 3 nozzle configurations have been designed and tested. These are the conical, equal-radii-of-curvature, and linear-velocity-profile nozzles shown in Fig. 6. These nozzles were designed for initial testing with a nozzle throat diameter which would provide a chamber Mach number of 0.05 and they were later remachined to provide a chamber Mach number of 0.10. The convergent sections of these nozzles are of equal length.

To determine the dependence of the number of ports used to exhaust a given flow rate, by a multiple-ported nozzle, upon nozzle damping 3 nozzle configurations were tested. These were the single-, dual-, and quadruple-ported nozzles shown in Fig. 7. These configurations have been designed to maintain identical total cross-sectional area variations along their convergent sections to ensure similar velocity distributions in their subsonic sections.

Results

To assure the repeatability of the experimental data, the admittance of the single-ported nozzle shown in Fig. 7(a) was measured in 2 separate tests. In Fig. 8, the frequency dependence of the parameter α obtained by measuring the standing wave pressure amplitudes and phases are presented. The mean square deviation between the 2 tests in the values of α obtained from pressure amplitude measurements is 0.007 and between those obtained from pressure phase measurements is 0.005. An examination of this figure also indicates that, though both measurement techniques yield comparable data, α obtained

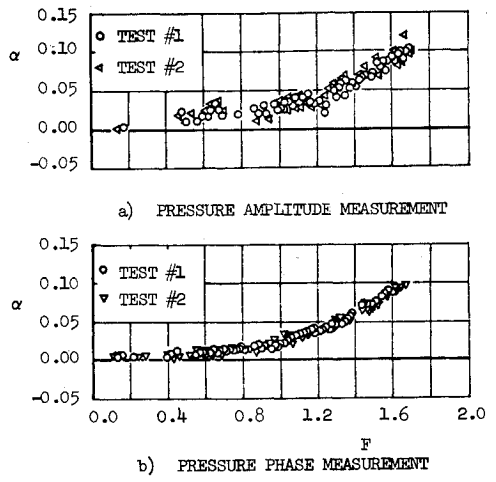

Fig. 8 Repeatability of admittance parameter α.

from pressure amplitude measurements has more scatter, particularly when α is very small, than the corresponding data obtained from pressure phase measurements. The same tests also established that pressure amplitude measurements yield β with less scatter than pressure phase measurements. The reasons for this observation are discussed in Ref. 14. The data presented in this paper on the submerged nozzle configuration were obtained from pressure amplitude measurements. The rest of the admittance data presented in this paper are based upon values of α obtained from phase measurements and values of β obtained from amplitude measurements.

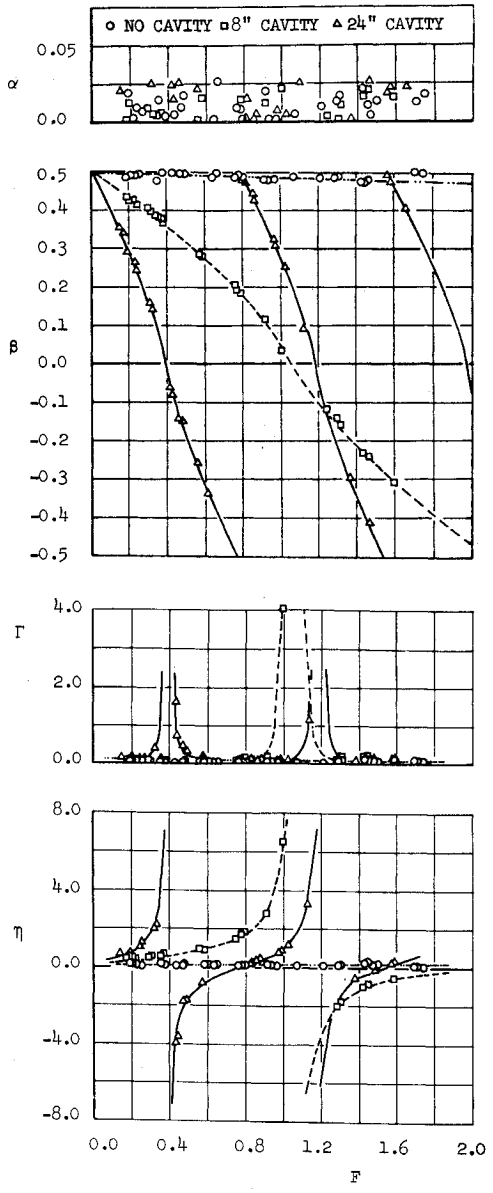

Fig. 9 Effect of cavity depth on admittance data of submerged nozzle with $q = 0$.

Submerged Nozzle

To determine the dependence of the submerged nozzle admittance upon the cavity depth and the secondary flow rate, the configuration shown in Fig. 5 was employed. Before presenting the data, some comments regarding the special geometrical features of the test configuration are in order. The situation can be best explained by referring to Fig. 5 and considering the unsteady flow conditions at the nozzle entrance plane. When a plane wave generated inside the modified impedance tube reaches the nozzle entrance plane it "splits" into two waves with one of them moving into the centrally-located nozzle and the other moving into the surrounding cavity. As a result, the local flow conditions at the nozzle entrance plane are nonuniform and the flow there cannot be one-dimensional. Hence the admittances measured in this study should be interpreted as effective one-dimensional admittances that describe average conditions across the nozzle entrance plane.

The dependence of the admittance parameters α and β and the nondimensional admittance of the submerged nozzle upon the cavity depth is presented in Fig. 9 and the dependence of the submerged nozzle admittance upon the cavity-to-chamber flow rate ratio is presented in Fig. 10. The data are presented as a function of the nondimensional frequency F, where $F = 2\pi f r_c/\bar{c}$.

Examination of the measured values of α obtained with a nozzle cavity present in the system shows that α is practically independent of the frequency and that its average value is close to the average value of α measured with no cavity present in the system. Examination of the measured values of β indicates that the magnitude of β is strongly affected by the depth of the cavity surrounding the nozzle. According to Eq. (6), the parameter β describes the phase difference at the nozzle entrance plane between the incident and the reflected pressure waves. When β is identically zero, the phase between the incident and reflected pressure waves equals to π radians. Such a phase difference is

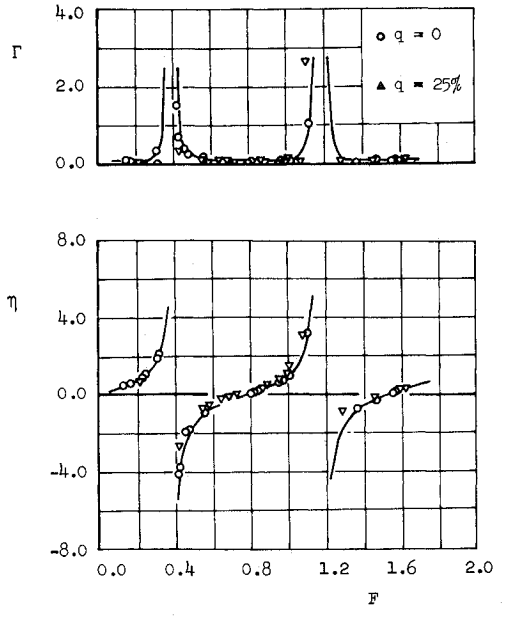

Fig. 10 Effect of cavity-to-chamber flow rate ratio on submerged nozzle admittance with 24″ cavity depth.

Table 1 Submerged nozzle cavity effect

L_{cavity} (in.)	q%	F (when $\beta = 0$)	α	L_{cavity}/λ
8	0	1.08	0.014	0.24
16	0	0.56	0.015	0.25
16	0	1.68	0.015	0.75
24	0	0.38	0.016	0.26
24	0	1.17	0.016	0.78
8	15	1.09	0.018	0.24
16	15	0.54	0.019	0.24
16	15	1.65	0.021	0.74
24	15	0.37	0.022	0.25
24	15	1.11	0.024	0.75
8	25	1.12	0.023	0.25
16	25	0.57	0.022	0.26
16	25	1.66	0.024	0.75
24	25	0.37	0.022	0.25
24	25	1.12	0.024	0.25

known to exist at the opening of a quarter-wave tube when the ratio of the tube length to the wavelength of the oscillation equals 0.25, 0.75, 1.25, and so on. To check whether the cavity surrounding the nozzle acts as a quarter-wave tube, the relationship $L_{cavity}/\lambda = L_{cavity}/(2\pi r_c/F)$ was used to compute the ratio of the cavity depth to the wavelength when the measured values of β were identically zero. The values of F for which $\beta = 0$ and the corresponding values of the ratio L_{cavity}/λ are presented in Table 1. The closeness of the computed values of L_{cavity}/λ to 0.25 and 0.75 shows that at the indicated frequencies the cavity surrounding the nozzle indeed behaves as a quarter-wave tube.

A further examination of Fig. 9 indicates that the behavior of the measured admittance is strongly dependent upon the cavity depth surrounding the nozzle. The latter observation is directly related to the strong dependence of β upon the cavity depth. It is also of interest to analyze the behavior of Γ, the measured real part of the nondimensional nozzle admittance. Examination of the data reveals that Γ becomes very large at values of F for which $\beta = 0$. In trying to explain this behavior one should recall the definition of the admittance and examine the structure of the acoustic wave in the chamber and the cavity. At frequencies for which the measured value of β is zero, the cavity acts as a quarter-wave tube and the amplitude of the pressure oscillation has a minimum value at the nozzle entrance plane. The observed values of Γ are caused by the fact that Γ is inversely proportional to the pressure amplitude. In connection with this observation it should also be pointed out that it would be misleading to conclude that the nozzle decay coefficient α_N is very large whenever Γ is very large. If one examines Eq. (19), one can see that α_N is proportional to the products $|P_N|^2\, Re\{y_N\}$ and $|P_N|^2\, |y_N|^2$, and due to the smallness of pressure amplitude $|P_N|$ these terms will be finite even though $Re\{y_N\}$ and $|y_N|$ are very large numbers. With the above observations in mind, one should be careful in using the real part of the admittance of a surface as the sole criterion for determining the attenuation or "driving" provided by this surface.

An examination of Fig. 10 shows that the nozzle admittance is practically independent of the cavity flow rate. However, when using Eq. (19) to calculate the nozzle decay coefficient for an engine with a submerged nozzle the fact that all the flow at the nozzle entrance plane is not unidirectional must be taken into consideration while performing the indicated spatial integration. An examination of Fig. 5 indicates that the secondary airflow from the cavity is flowing in a direction opposite to that of the primary airflow and hence is "convecting" acoustic energy from the cavity into the chamber. The effect of the secondary airflow on the nozzle decay coefficient is discussed in greater detail in Ref. 14.

The conclusions that follow from this study on submerged nozzles are: a) the cavity depth surrounding the submerged nozzle has a significant effect upon the nozzle admittance, b) the secondary flow rates issuing from the cavity have negligible effect on the nozzle admittance, and c) the presence of a "reversed" cavity flow at the nozzle entrance plane should be suitably taken into consideration while calculating the decay coefficient for a combustor with a submerged nozzle.

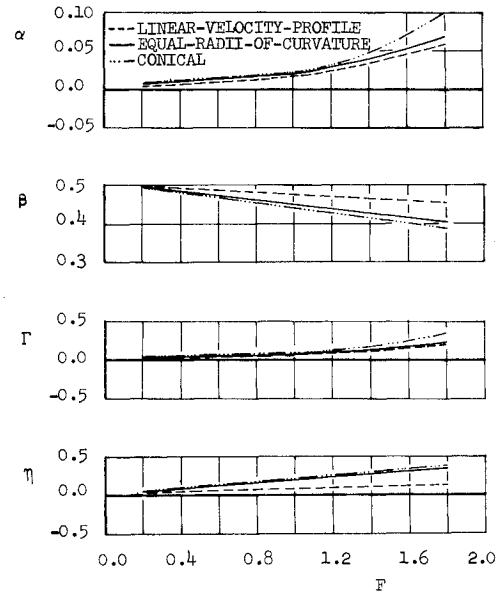

Fig. 11 Effect of nozzle geometry upon admittance data.

Nozzle Geometry

The acoustic losses associated with a rocket nozzle of a given contraction ratio depend upon the geometry of the nozzle convergent section and the manner in which the nozzle is attached to the combustor. To determine the dependence of the damping of solid rocket nozzles upon the geometry of the nozzle convergent section, the damping provided by a conical, an equal-radii-of-curvature and a linear-velocity-profile nozzle (i.e., see Fig. 6) was measured with chamber Mach numbers of 0.05 and 0.10. The admittance data obtained with a chamber Mach number of 0.10 is presented in Fig. 11.

To evaluate the relative damping capabilities of the tested nozzle configurations, the nozzle decay coefficient was calculated using the measured admittance data. To obtain an expression for the evaluation of α_N, the real and imaginary parts of p_1 and u_1, obtained from Eqs. (1) and (2), were substituted into Eqs. (16) and (17) and the indicated integrations were performed. The resulting expression for the nondimensional nozzle decay coefficient Λ_N is:

$$\Lambda_N = \frac{\alpha_N L_c}{\bar{c}} = -\frac{\bar{M} + [(1+\bar{M}^2)/2]\tanh(2\pi\alpha)}{1+\bar{M}\tanh(2\pi\alpha)} \qquad (20)$$

Employing the measured values of the admittance parameter α and Eq. (20) the nondimensional decay coefficients of the tested nozzles were calculated and the results are presented in Fig. 12. The error associated with the calculated values of Λ_N can be determined using the observed mean square deviation in the measured values of α and Eq. (20). When both $\bar{M}$ and α are small quantities, Eq. (20) reduces to $\Lambda_N = -(\bar{M} + \pi\alpha)$. Using this relation and the observed mean-square deviation of 0.005 in the values of α, the deviation in values of Λ_N are found to be approximately equal to 0.016.

An examination of the measured values of α and Γ and the calculated values of Λ_N leads to the following observations. At a given chamber Mach number all the 3 nozzle configurations provide approximately the same damping for axial instabilities in the low frequency range. For nondimensional frequencies F greater than approximately 1.0 the difference in the damping capabilities of the 3 nozzle configurations becomes more

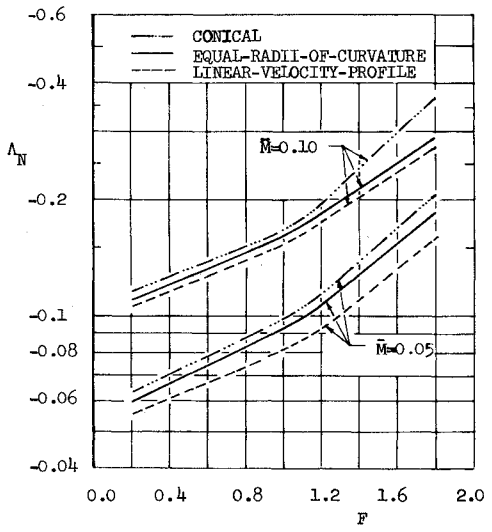

Fig. 12 Effect of nozzle geometry upon nozzle decay coefficient.

apparent. For a given entrance Mach number, the conical nozzle provides more damping than the equal-radii-of-curvature nozzle which provides more damping than the linear-velocity-profile nozzle. Examination of the measured values of β and η indicates that the conical nozzle causes a larger phase shift at the nozzle entrance, between the incident and reflected pressure waves, than the equal-radii-of-curvature nozzle which produces a larger phase shift than the linear-velocity-profile nozzle. These differences in phase shift indicate that the conical nozzle "appears" to the oscillations in the chamber as being "longer" than the equal-radii-of-curvature and linear-velocity-profile nozzles.

A further examination of Fig. 12 indicates that the behavior of log Λ_N exhibits two distinct trends depending upon the value of F; the transition between these trends occurs at a value of F between 1.0 and 1.2. When F equals 1.0 the wavelength of the oscillation in the impedance tube approximately equals 36 in. By taking the ratio of the length of the convergent section of the nozzles tested in this study to the above value of λ, one obtains $L_N/\lambda \approx 0.1$. In light of the preceding discussion and from an examination of the measured data it appears that the admittances of nozzles tested in this study are practically independent of the frequency when the condition $L_N/\lambda < 0.1$.

Table 2 Empirical relations for Λ_N

Nozzle	Λ_N	
	$\bar{M} = 0.05$	$\bar{M} = 0.10$
Linear-velocity-profile	$-\frac{5.1}{100-38F}$	$-\frac{9.6+1.5F}{100-30F}$
Equal-radii-of-curvature	$-\frac{5.4+0.6F}{100-38F}$	$-\frac{10+1.2F}{100-32F}$
Conical	$-\frac{5.8+0.58F}{100-37F}$	$-\frac{11-F}{100-42F}$

In order to assess the effect of the Mach number on the damping capabilities of the nozzles tested in this study, the admittance data for the conical nozzle obtained with chamber Mach numbers of 0.05 and 0.10 were plotted and the data are presented in Fig. 13. An examination of this figure indicates that increasing the Mach number from 0.05 to 0.10 has little effect on the values of the α and Γ for all values of F less than approximately 1.0 (or $L_N/\lambda < 0.1$). For values of F greater than 1.0 (or $L_N/\lambda > 0.1$), an increase in the Mach number from 0.05 to 0.1 results in a small increase in values of α and Γ. The above observations regarding the effect of increasing the mean flow Mach number on the damping of the conical nozzle also apply to the equal-radii-of-curvature and the linear-velocity-profile nozzles. These results seem to indicate that the admittances of solid rocket nozzles may be practically independent of the mean flow Mach number for values of $L_N/\lambda < 0.1$. On the other hand the magnitudes of α and Γ slightly increase with increase in Mach number for all values of $L_N/\lambda > 0.1$.

To facilitate the use of the measured data in the design of solid rockets, rational functions were used to derive empirical relationships that describe the frequency dependence of Λ_N. The derived empirical expressions are presented in Table 2. The error associated with these relations, when compared with the data of Fig. 12, is between 2% and 5%.

The main conclusion of this study is that the conical nozzle provides more damping than the equal-radii-of-curvature nozzle which in turn provides more damping than the linear-velocity-profile nozzle. Hence, for a given solid rocket nozzle with fixed values of entrance diameter, throat diameter, and length of the convergent section, the damping capability of the nozzle can be

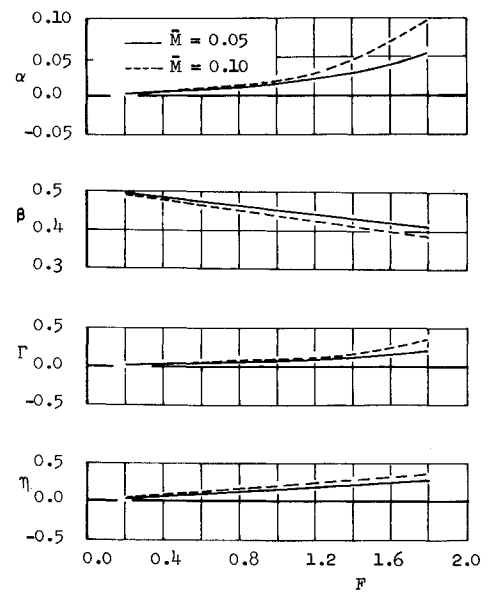

Fig. 13 Effect of mach number on admittance data of conical nozzle.

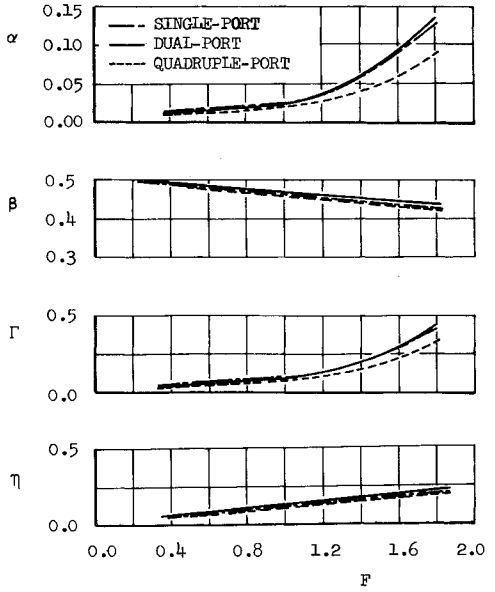

Fig. 14 Effect of number of nozzle ports on admittance data.

increased by suitably redesigning the geometry of its convergent section, particularly for values of F greater than 1.0. Finally, the admittances of solid rocket nozzles are "weakly" dependent upon the frequency and chamber Mach number for values of $L_N/\lambda < 0.1$ and they increase with frequency and Mach number for large values of the preceding ratio.

Multiple Nozzle Clusters

To investigate the dependence of damping provided by multiple nozzle clusters upon the number of nozzles present in the nozzle cluster, tests were conducted using the single-, dual-, and quadruple-nozzle configurations shown in Fig. 7. The measured admittance data are presented in Fig. 14. An examination of the measured values of α and Γ shows that the quadruple-ported nozzle provides less damping for axial instabilities than the single- and dual-ported nozzles. The difference in the damping capabilities of these three nozzle configurations is particularly apparent at nondimensional frequencies larger than 1.0. It is also noted from this figure that the single- and dual-ported nozzles provide approximately the same damping. Examination of the measured values of β and η indicates that all 3 nozzle configurations result in approximately the same phase shift at the nozzle entrance plane between the incident and reflected pressure waves.

The main conclusion of this study is that the quadruple-ported nozzle provides less damping for axial instabilities than the single- and dual-ported nozzles whose damping capabilities are approximately the same.

References

[1] Price, E. W., "Experimental Solid Rocket Combustion Instability," *Tenth Symposium (International) on Combustion*, The Combustion Institute, Pittsburgh, Pa., 1965, pp. 1067–1082.

[2] Bergman, G. H. and Jessen, E. C., "Evaluation of Conventional Rocket Motor Instabilities for Analysis of Oscillatory Combustion," AIAA Paper 71–755, Salt Lake City, Utah, 1971.

[3] Browning, S. C., Krashin, M., and Thacher, J. H., "Application of Combustion Instability Technology to Solid Propellant Rocket Motor Problems. "*Journal of Spacecraft and Rockets*, Vol. 9, No. 5, May 1972, pp. 293–294.

[4] Crocco, L. and Sirignano, W. A., *Behavior of Supercritical Nozzles under Three-Dimensional Oscillatory Conditions*, AGARDograph 117, Butterworth, London, 1967.

[5] Crocco, L. and Sirignano, W. A., "Effect of Transverse Velocity Components on the Nonlinear Behavior of Short Nozzles," *AIAA Journal*, Vol. 4, No. 8, Aug. 1966, pp. 1428–30.

[6] Zinn, B. T., "Longitudinal Mode Acoustic Losses in Short Nozzles," *Journal of Sound and Vibration*, Vol. 22, No. 1, May 1972, pp. 93–105.

[7] Crocco, L., Monti, R., and Grey, J., "Verification of Nozzle Admittance Theory by Direct Measurement of the Admittance Parameter," *ARS Journal*, Vol. 31, June 1961, pp. 771–775.

[8] Buffum, R. G., Dehority, G. L., Slates, R., and Price, E. W., "Acoustic Attenuation Experiments on Subscale Cold-Flow Rocket Motors," *AIAA Journal*, Vol. 5, No. 2, Feb 1967, pp. 272–280.

[9] Beranek, L. L., *Acoustic Measurements*, Wiley, New York, 1949.

[10] Culick, F. E. C. and Dehority, G. L., "Analysis of Axial Acoustic Waves in a Cold-Flow Rocket," *Journal of Spacecraft and Rockets*, Vol. 6, No. 5, May 1969, pp. 591–595.

[11] Bell, W. A., "Experimental Determination of Three-Dimensional Liquid Rocket Nozzle Admittances," Ph.D. thesis, School of Aerospace Engineering, Georgia Institute of Technology, Atlanta, Ga., 1972.

[12] Zinn, B. T., Bell, W. A., Daniel, B. R., and Smith, A. J., "Experimental Determination of Three-Dimensional Liquid Rocket Nozzle Admittances," *AIAA Journal*, Vol. 11, No. 3, March 1973, pp. 267–272.

[13] Morse, P. M. and Ingard, K. U., *Theoretical Acoustics*, McGraw-Hill, New York, 1968.

[14] Zinn, B. T., Daniel, B. R., Janardan, B. A., and Smith, A. J., Jr., "Nozzle Design Considerations for Attenuation of Axial Instabilities in the Minuteman II and III, Stage III, Rocket Motors," AFRPL-TR-73-69, Sept. 1973.

[15] Coates, R. L. and Horton, M. D., "Design Considerations for Combustion Instability," *Journal of Spacecraft and Rockets*, Vol. 6, No. 3, March 1969, pp. 296–302.

[16] Cantrell, R. H. and Hart, R. W., "Interaction Between Sound and Flow in Acoustic Cavities; Mass, Momentum and Energy Considerations," *Journal of the Acoustic Society of America*, Vol. 36, No. 4, April 1964, pp. 697–706.